Direct Ocean Disposal of Carbon Dioxide, edited by N. Handa and T. Ohsumi, pp. 23–34.

The Role of the Pacific Ocean as a Regulator of Atmospheric Carbon Dioxide Concentrations

Chen-Tung Arthur Chen

Institute of Marine Geology, National Sun Yat-Sen University, Kaohsiung, Taiwan, Republic of China

Abstract. The oceans contain an amount of dissolved carbon over 50 times that present in the atmosphere and have acted as a major regulator of atmospheric carbon dioxide concentrations. The surface wind-mixed layer (less than 200 m deep) of most of the oceans is more or less saturated with excess CO_2. The deep waters (from 200 m to an average depth of 3800 m), on the other hand, have not been affected by the excess CO_2 except near their source regions, such as the northern North Atlantic Ocean, the Red Sea, and the Weddell Sea. This slow penetration of excess CO_2 into the deep waters is due to the slow exchange of waters across the thermocline that separates the surface and deep waters. More and more excess CO_2, however, will gradually penetrate into the deep oceans. I examine this process by discussing the excess CO_2 signal in the Pacific Ocean, and comparing the signal with signals of transient tracers. The Bering Sea is found to contain $0.19 \pm 0.05 \times 10^{15}$ g excess carbon. The North and South Pacific Oceans contain, respectively, 14.5 ± 4 and $16.6 \pm 4 \times 10^{15}$ g excess carbon.

1. Introduction

The oceans cover around 60% of the surface in the Northern Hemisphere and over 80% in the Southern Hemisphere. Overall, the oceans cover 70.8% of Earth's surface and are the giant of carbon dioxide control. There is 20 times more carbon dissolved in seawater than occurs on land (in biota and soil). The oceans' CO_2 reservoir is more than 50 times the size of the atmospheric CO_2 reservoir and the release of just 2% of the carbon stored in the oceans would double the level of atmospheric CO_2. Furthermore, each year around 15 times more CO_2 is taken up and released by natural marine processes than the total produced by the burning of fossil fuels, deforestation and other human activities[1].

The amounts of CO_2 entering and leaving the oceans over an annual cycle are usually close to global balance. However, air-sea exchanges are controlled by many different processes with large special and temporal variations[2]. Circulation patterns and other physico-chemical conditions govern CO_2 solubility, gas transfer rates across the sea surface, and the bulk transport of carbon within the

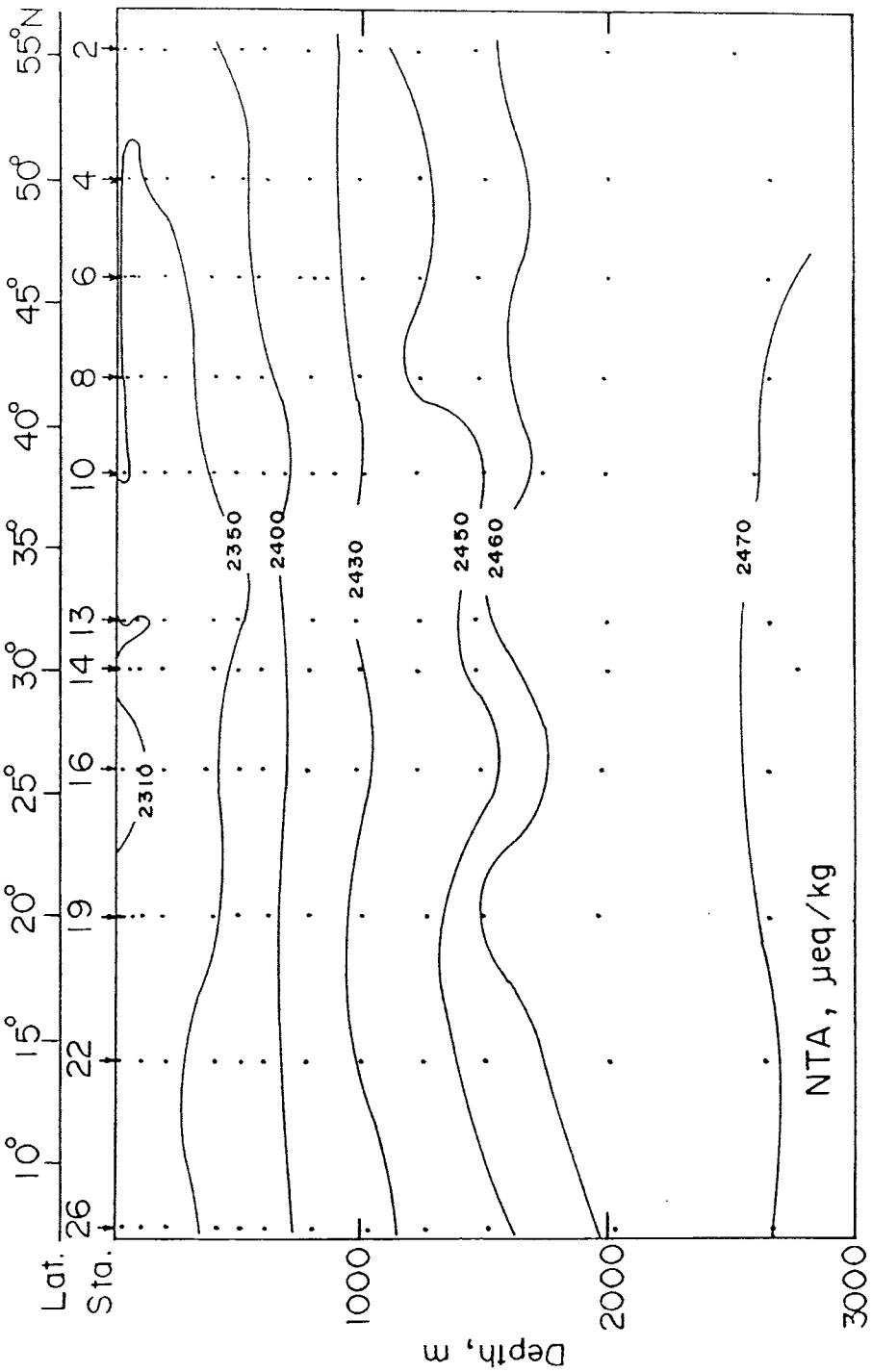

Fig. 1. Cross-section of normalized alkalinity along 150°W in the North Pacific.

oceans. Superimposed on (and strongly influenced by) these effects are two basic biological processes: carbon fixation by photosynthesis, and CO_2 release by respiration[1]. As a result, the surface ocean is rarely in equilibrium with the atmospheric CO_2.

Photosynthesis is limited to the sunlit, upper ocean while respiration occurs throughout the water column. Over geological periods of time, marine plankton have been responsible for a vast accumulation of carbon in the oceans and in sediments, altering atmospheric composition. Biological and physical CO_2 "pumps" remove CO_2 from surface water and release it in the deep ocean thereby providing the main driving forces for the ocean carbon cycle. At present, only the broad outline is known, with physical CO_2 uptake occurring mostly in sub-polar regions (particularly the North Atlantic) and CO_2 release mostly in equatorial regions (particularly the Pacific). Those features closely match the pattern of global ocean circulation, with surface water cooling and sinking in the former regions, and deep water upwelling and warming in the latter. Lateral movements of waters complete the physical ocean "conveyor belt" for the transport of carbon around the world[1].

Biological CO_2 pumps are more vertically-directed, promoting the transfer of carbon from surface to deep ocean (Fig. 1). Several pathways are involved: the sinking of plant and animal debris, containing both organic carbon and calcium carbonate; active downward transport, brought about by the feeding and excretory behavior of migratory zooplankton; and the downward advection and diffusion of dissolved organic carbon, produced mainly by decomposition processes in the upper ocean[1].

The net effect of such biological activity is to reduce pCO_2 in surface waters, causing the drawdown of CO_2 from the atmosphere. Its rate of return is subsequently determined by the depth distribution of respiration and decomposition processes, and by physical factors influencing carbon transport in the water column[1].

We cannot yet, however, measure the components of the global carbon cycle with sufficient accuracy to balance the carbon budget[1),(3)]. While it is known that human activities add 5–6 giga (10^9) tonnes of carbon each year to the atmosphere, the annual increase in atmospheric CO_2 is equivalent to only 3 giga tonnes of carbon. We do not yet have an accurate account of where the remaining 2–3 giga tonnes of carbon go. Quantifying and balancing carbon circulation processes in different oceans, and for the world as a whole, is a major aim of the JGOFS program.

2. Oceanic Excess CO_2 Penetration

Recently it has been shown that the oceanic penetration of excess (anthropogenic) CO_2 can be calculated using carbonate data. Because the method is subject to large uncertainties, the accuracy of the results is not known. However, the

precision of the method is adequate to show the excess CO_2 signal. The abundant carbonate data in the literature can thus be used to supplement the tracer data in showing oceanic mixing features for waters formed in the last 130 years[3]–[16].

The method of computation and its limitations have been described in detail elsewhere[5]–[18]. The method involves a back-calculation of the CO_2 concentration of a parcel of seawater to its initial concentration at the sea surface by correcting for changes due to the decomposition of organic material and dissolution of carbonate particulates. These back-calculated CO_2 concentrations of waters with various ages are then compared with each other and with the contemporary surface CO_2 concentrations to obtain the oceanic CO_2 increase.

3. Excess CO_2 Penetration along the 150°W Cross-Section in the North Pacific

Figure 2 shows the results of fossil-fuel CO_2 penetration along the 150°W

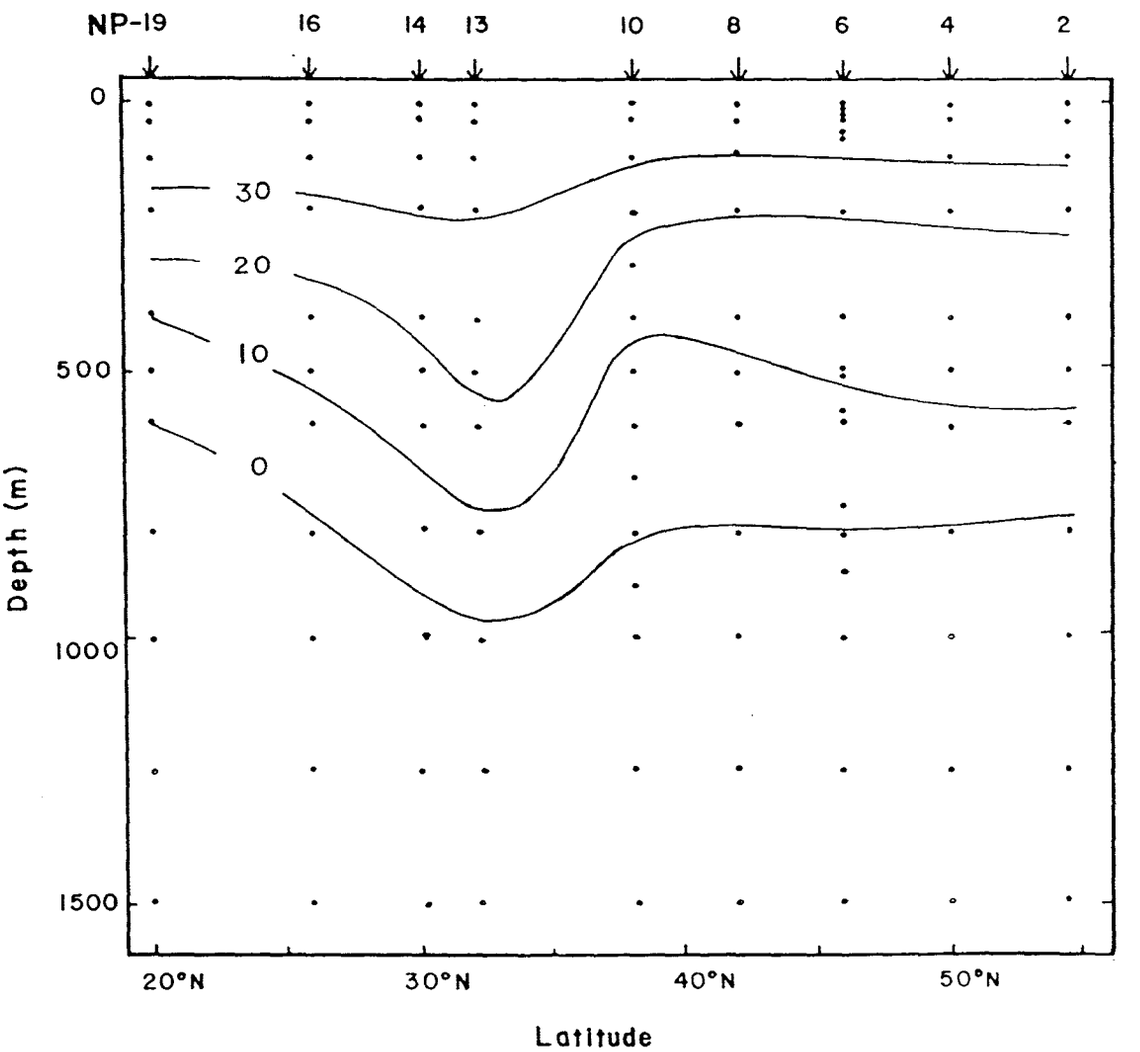

Fig. 2. Cross-section of excess CO_2 (μmol/kg) along 150°W.

cross-section in the North Pacific[5]. The waters underlying the 0 μmol/kg excess CO_2 contour are free from fossil fuel CO_2. The increasing excess CO_2 from the deep to the surface layer indicates that the fossil-fuel CO_2 content is greater in the shallow water than in the deep water. I proposed that the deepening of penetration depth at 30°N is not a local phenomenon but is an advected feature derived from the northwest North Pacific. Local convergence in the winter only brings surface water to approximately 300 m.

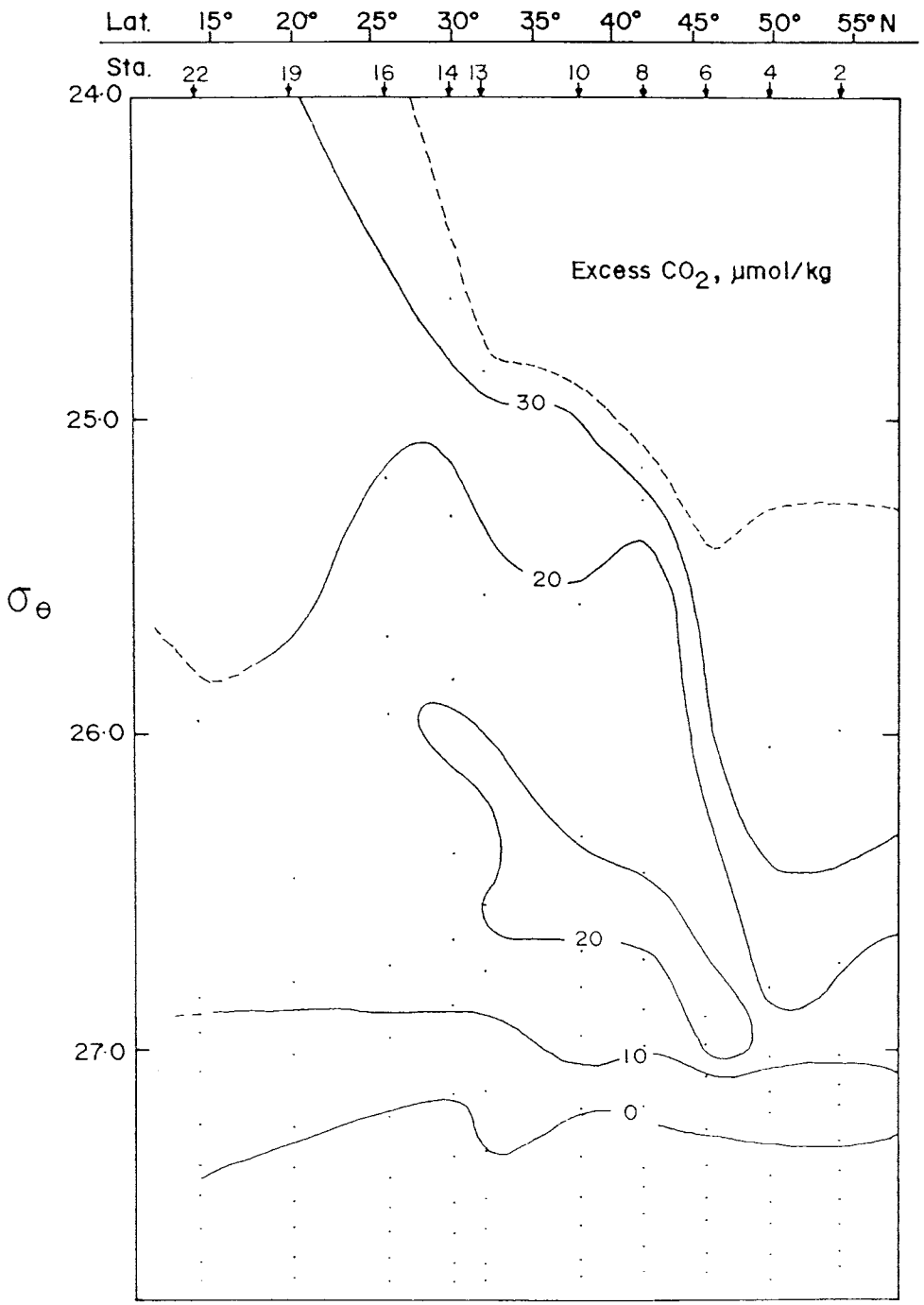

Fig. 3. Excess CO_2 vs. σ_θ along 150°W.

The values of excess CO_2 plotted vs. σ_θ in Fig. 3 cannot be contoured in detail but nevertheless provide supporting information[14]. The isopleths less than 10 μmol/kg are relatively flat and the 0 μmol/kg contour which is indicative of the oldest water is at or below ~27.2σ_θ throughout the section. At values greater than 10 the distribution is very non-isopycnal, with a value greater than 20 centered in the deep S-min layer, indicating that younger water is associated with these strata. Since this water originates in the northwest Pacific as a result of near surface processes, this higher excess CO_2 indicates more recent surface origin. In the vicinity of the subarctic front near 45°N the strongest north-south gradient exists and extends to depths of about 600 m and σ_θ of 27.00. Between 50°N and 40°N the 20 μmol/kg isopleth shallows from the 26.80σ_θ isopleth to the 25.5σ_θ isopleth, suggesting that vertical processes are able to rejuvenate the water north of the subarctic front more effectively than south of this front.

The 26.8σ_θ density surface was chosen by Fine *et al.*[19] as the lower boundary of the intermediate layer containing the most tritium in the North

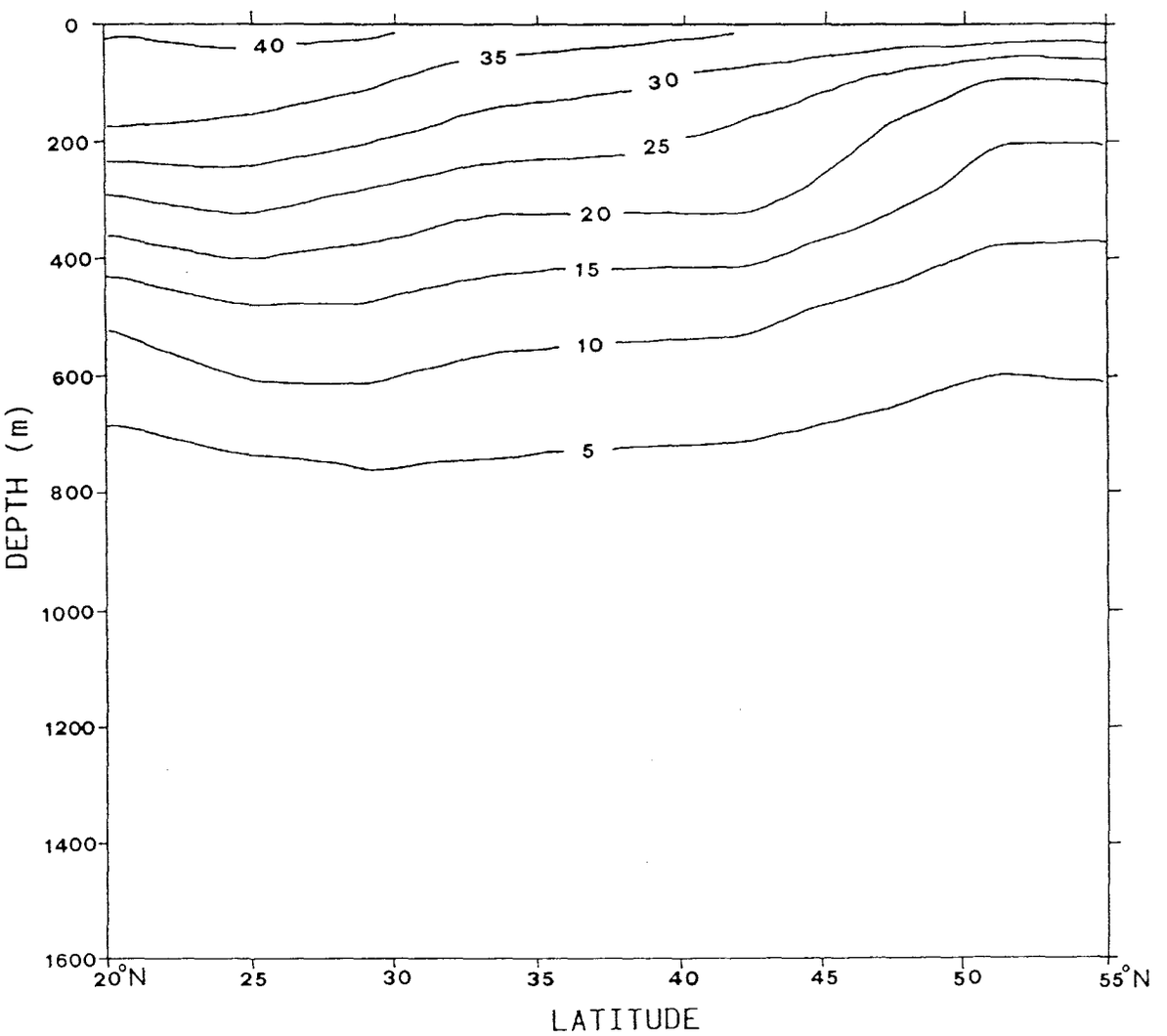

Fig. 4. The 3-D model calculated excess CO_2 (μmol/kg) redrawn from Sarmiento *et al.* [22].

Pacific. Evidently excess CO_2 has penetrated much deeper than this level. Fine *et al.* used $26.8\sigma_\theta$ because it was just below the maximum outcrop density for the winter North Pacific and thus diffusion downward from the mixed layer and lateral ventilation along outcrops provided a direct atmospheric link. The depth of this surface was from 800 m at 30°N in the western North Pacific to 150 m further north and 300 m in the equatorial regions. For the 150°W section presented here the depth of this isopycnal is generally near 500 m and somewhat deeper near 30°N as part of the geostrophic response to the subtropical gyre. There is also some indication that the center of the gyre shifts northward due to the northward progression of deepest penetration for each isopycnal. It is important to note that significant tritium is found below this surface despite no direct atmospheric links having been established.

Excess CO_2 vs. salinity distribution for the 150°W section indicates that less excess CO_2 is associated with higher salinities. The waters at salinities less than approximately 34.5, therefore, must be receiving a younger input. The salinity where the deep water θ/S curves converge is near or less than 34.6. Thus the younger waters are also associated with fresher water. The source regions are believed to be in the Northwest Pacific where intermediate water formation occurs and where vertical mixing, mode water formation and thermocline ventilation appear to be most enhanced[20),(21)].

Recently Sarmiento *et al.*[22] simulated the uptake of excess CO_2 by the ocean using a perturbation approach in a 3-dimensional global general circulation model. Figure 4 shows results of the 3-D model-predicted excess CO_2 at 150°W. The 3-D model results in a penetration pattern similar to that obtained by using carbonate data directly. The structure, however, is somewhat different. The carbonate-derived results show a deepening of the penetration depth at 30°N while this feature is lacking in the 3-D model. These differences may reflect problems in the 3-D model's thermocline ventilation[22].

4. Isogram Map of Excess CO_2 in the Pacific Ocean

An isogram map of the lower boundary of the excess CO_2 penetration in the Pacific Ocean is shown in Fig. 5. Excess CO_2 does not penetrate below the thermocline in the Pacific Ocean because there is no bottom water formation in the North Pacific[8]. The shallowest penetration outside of the Southern Ocean occurs in the eastern equatorial region where the excess CO_2 only penetrates to 400 m, or shallower. Because few data are available for the complex oceanic region in the western equatorial Pacific, results there are less reliable. The general trend, however, indicates a deeper penetration (800 m) in the western Pacific and in the South China Sea[9),(23)]. Overall, the excess CO_2 penetrates to a shallower depth in the equatorial Pacific than in the Atlantic[6),(8)] and Indian Ocean[9),(23)], perhaps reflecting the higher equatorial upwelling rate in the Pacific and less influence of the newly formed water advected from the North[9),(24)].

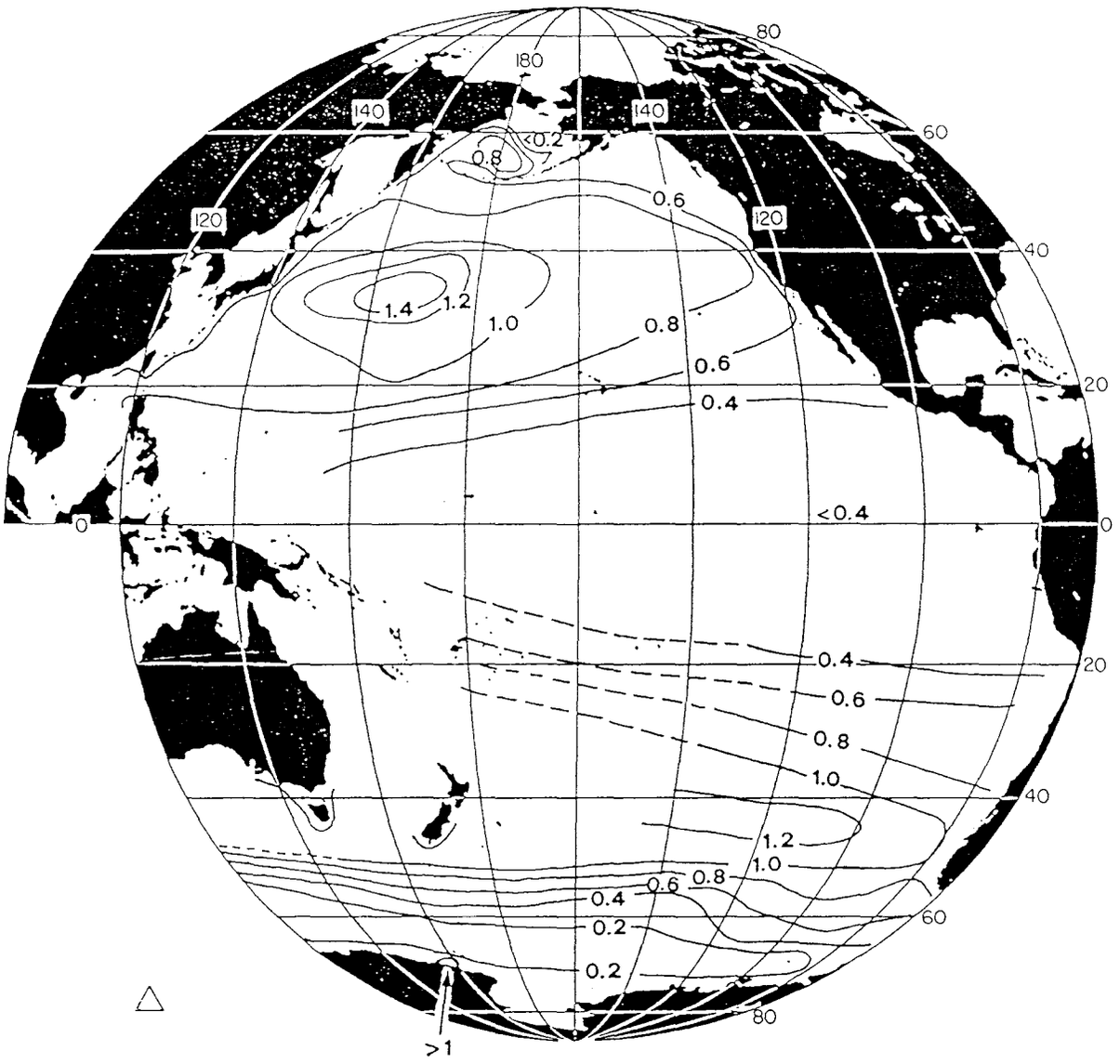

Fig. 5. Isogram of the lower boundary of excess CO_2 penetration (km) in the Pacific Ocean.

Similar to what was found in the weddell Sea[8], intensive upwelling prevents excess CO_2 from reaching more than 200 m deep in the region around 65°S. The excess CO_2 penetrates deeper further south, and reaches more than 1000 m off Cape Adare at the northwest corner of the Ross Sea[8].

The deepest excess CO_2 penetration in the South Pacific occurs around 45°S near where the Subantarctic Mode Water is located, but the depth of penetration is slightly shallower than that found in the South Atlantic Ocean. Intensive vertical mixing in the Drake Passage also seems to result in deeper excess CO_2 penetration compared to the situation found elsewhere at the same latitude. The deepest penetration in the North Pacific occurs in the confluence of the Kuroshio and Oyashio currents. This is the region off Japan near the area of circulation of the North Pacific variety of the Subtropical Mode Water. Here excess CO_2 has penetrated to a depth of more than 1400 m (Fig. 5). In general, deeper penetration

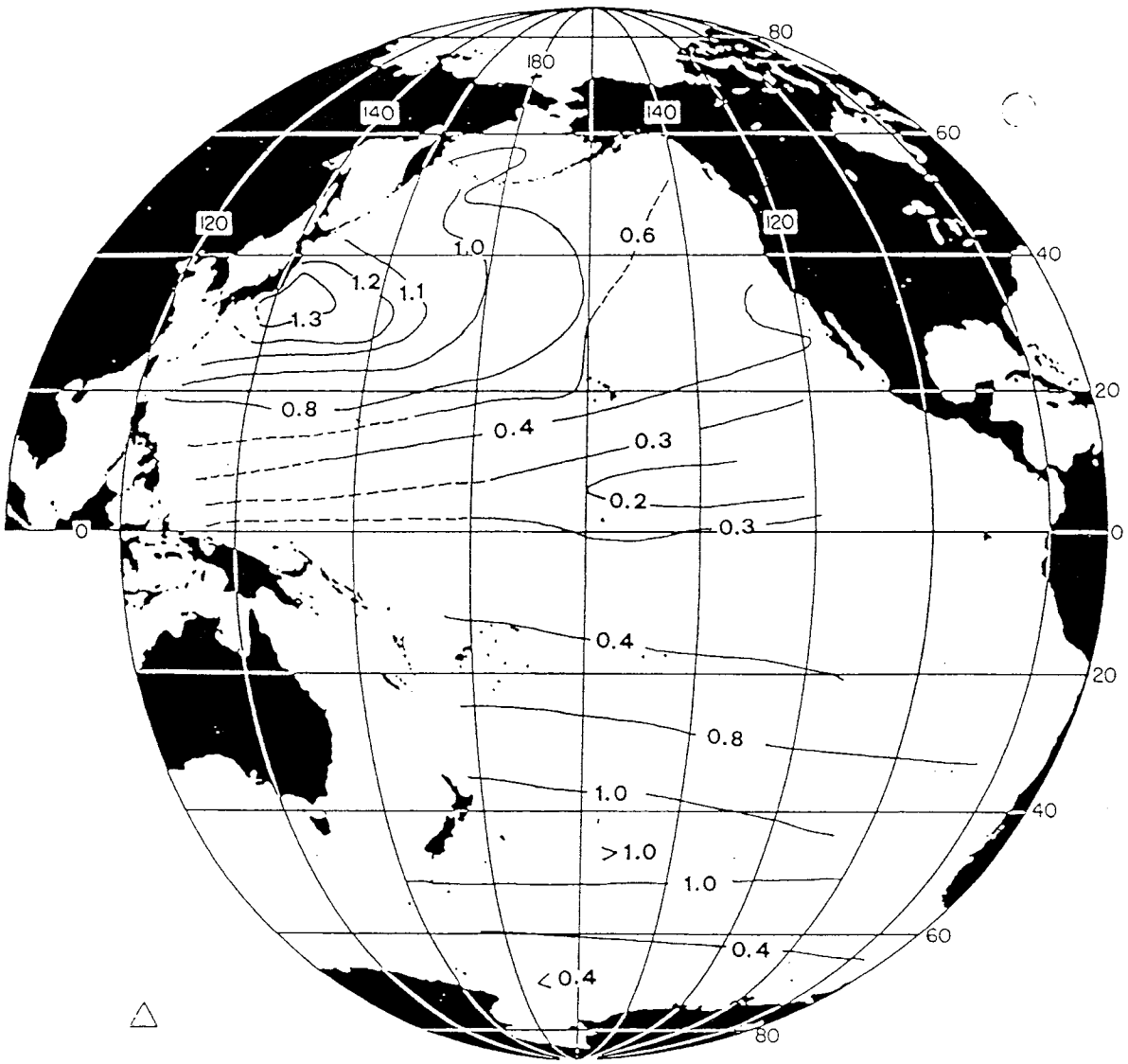

Fig. 6. Isogram of the lower boundary (km) of tritium penetration in the Pacific Ocean[25],[26].

occurs on the western side of the Pacific[3],[9].

Figure 6 is an isogram map of the depth where tritium equals to 0.1 TU[25],[26]. The similarity in distribution with the excess CO_2 results is striking. Few tritium data exist, however, south of 65°S so I do not know whether tritium penetrates deeper near the Antarctic Continent.

Based on the oceanic seawater data[27],[28], and the coral data[29],[30] the pre-industrial ΔC-14 concentration for low and mid-latitude waters in the Pacific Ocean is probably about –50‰, similar to the value in the Atlantic Ocean. Figure 7 shows an isogram map of the depth where the ΔC-14 concentration equals to this value[25],[31]. The agreement with the excess CO_2 results is rather good between 30°S and 30°N. At higher latitudes the agreement is poor because the subsurface waters in the Subarctic and Antarctic regions have a pre-industrial ΔC-14 concentration near –110‰[27],[28],[30]. Figure 8 shows an isogram map of the depth at

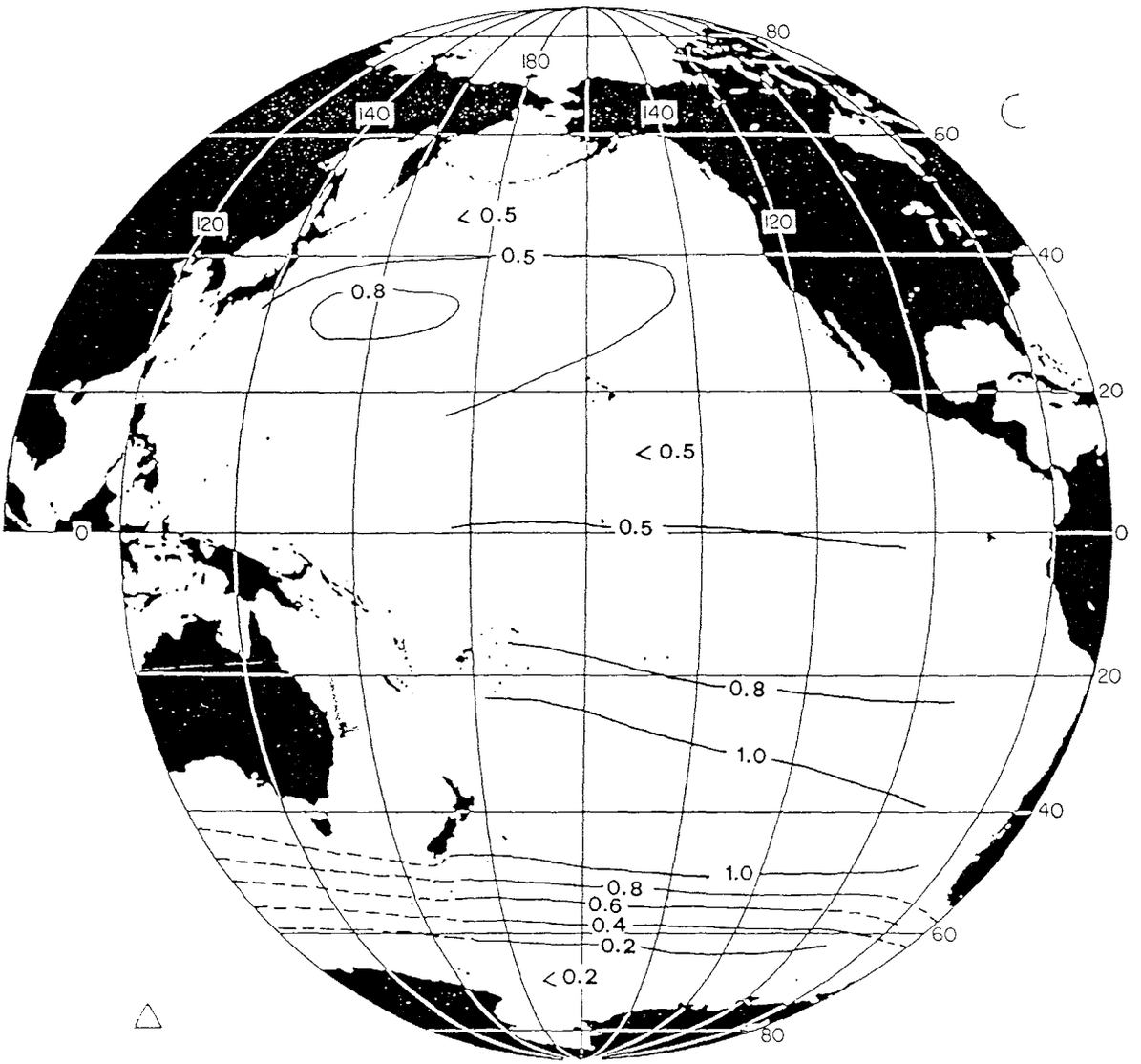

Fig. 7. Isogram of the depth (km) in the Pacific Ocean where the ΔC-14 concentration equals −50‰[25],[31].

which ΔC-14 equals −110‰. The results north of 30°N and south of 30°S agree better with the excess CO_2 results shown in Fig. 5, but near equator the excess CO_2 has not reached the depth where ΔC-14 equals −110‰[8]. Note that tritium and C-14 are all transient tracers thus the signals detected have a temporal variability[32]. It is important to keep in mind that the above comparisons often involve data collected in different years and should not be considered quantitative.

It is now possible to integrate the amount of excess CO_2 contained in each ocean. The Bering Sea has been estimated to contain $0.19 \pm 0.05 \times 10^{15}$ g excess carbon around 1980[33]. The North Pacific Ocean (excluding the Bering Sea) and the South Pacific Ocean contained 14.5 ± 4 and $16.6 \pm 4 \times 10^{15}$ g excess carbon respectively around 1980[9]. Overall the Pacific Ocean contained $31.3 \pm 6 \times 10^{15}$ g excess carbon, less than found in the Atlantic Ocean despite of the much larger capacity[9].

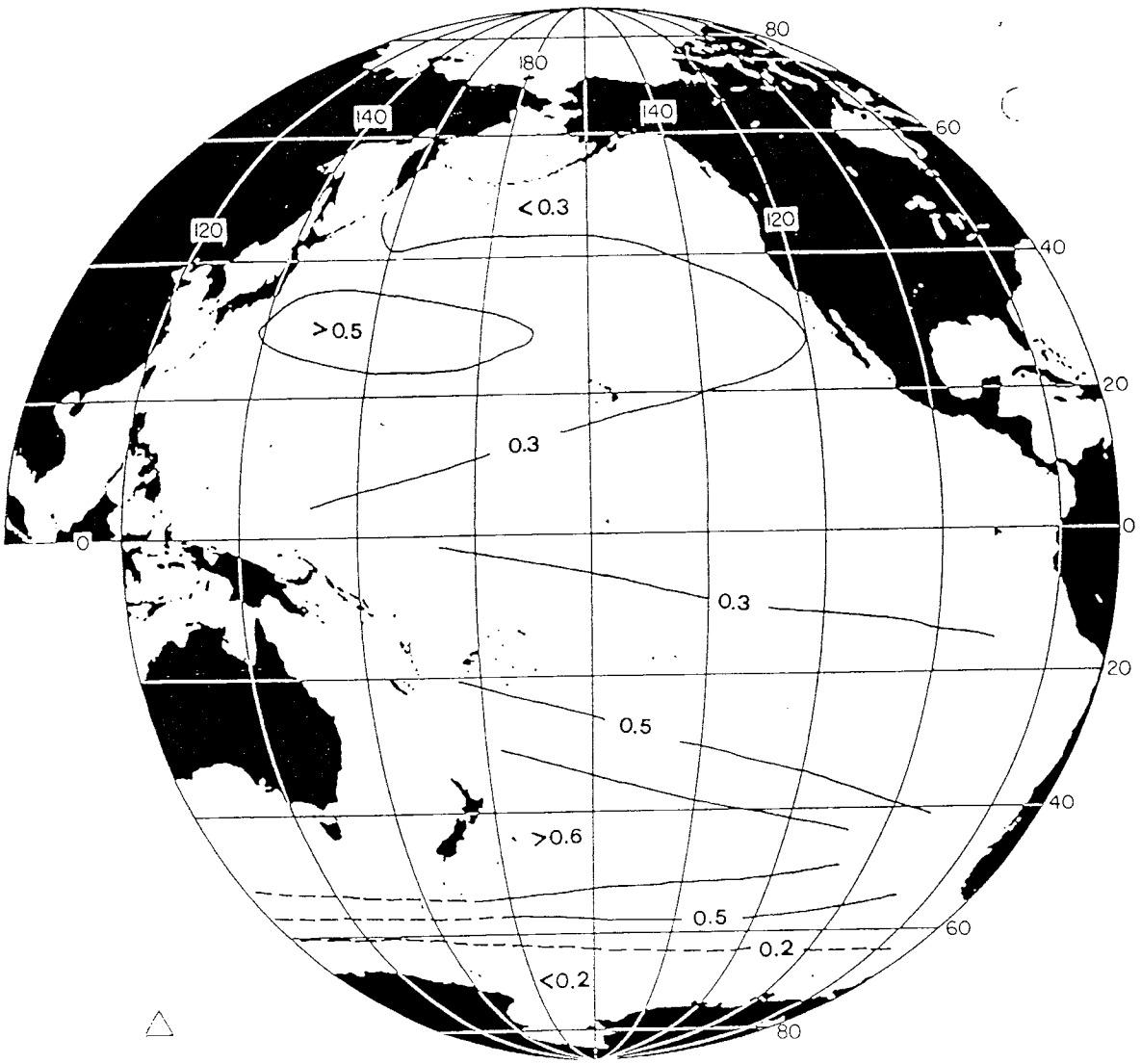

Fig. 8. Isogram of the depth (km) in the Pacific Ocean where the ΔC-14 concentration equals −11‰[25],[31].

5. Conclusion

The lower boundary of anthropogenic CO_2 penetration based on carbonate data in the literature has been shown for the Pacific Ocean. The results indicate that the distribution of excess, anthropogenic CO_2 follows the large-scale movements of water masses such as vertical mixing, upwelling, and Mode Water formation. The deepest penetration is found in the areas where the Subtropical Mode Waters are found: the northwest Pacific off Japan, and around 45°S. The shallowest penetration areas are around 65°S and in the eastern equatorial region. Overall the Pacific Ocean contains $31.3 \pm 6 \times 10^{15}$ g excess carbon around 1980.

Acknowledgements. I thank NSC (81-0209-M110-01) for its financial support.

REFERENCES

(1) Scientific Committee on Oceanic Research. 1990. An introduction to JGOFS, 12 pp.
(2) Inoue, H., Y. Sugimura and K. Fushimi. 1987. *Tellus*, **39B**, 228–242.
(3) Chen, C. T. A. 1991. Proceedings, Asian Workshop on the IGBP—a Study of Global Change, IGBP Report 18.2, in press.
(4) Brewer, P. G. 1978. *Geophys. Res. Lett.*, **5**, 997–1000.
(5) Chen, C. T. 1982. *Geophys. Res. Lett.*, **9**, 117–119.
(6) Chen, C. T. 1982. *Deep-Sea Res.*, **29**, 563–580.
(7) Chen, C. T. and F. J. Millero. 1978. *EOS*, **59**, 1101.
(8) Chen, C. T. A. 1987. *Oceanological Acta*, No. sp, 97–102.
(9) Chen, C. T. A. 1991. Regional Workshop on the Carbon Cycle and Global Climate Change, UNESCO/UNEP/IHP/DOE, Kuala Lumpa, Malaysia.
(10) Chen, C. T. and F. J. Millero. 1979. *Nature*, **277**, 205–206.
(11) Chen, C. T. and R. M. Pytkowicz. 1979. *Nature*, **281**, 362–365.
(12) Chen, C. T., F. J. Millero and R. M. Pytkowicz. 1982. *J. Geophys. Res.*, **87**, 2083–2085.
(13) Chen, C. T. A., E. D. Jones and K. J. Lin. 1990. *Deep-Sea Res.*, **37**, 1455–1473.
(14) Chen, C. T., M. R. Rodman, C. L. Wei and E. J. Olson. 1986. U.S. Department of Energy DOE/NBB-0079, 176 pp.
(15) Cline, J. D., R. A. Feely, K. Kelly-Hansen, J. F. Gendron, D. P. Wisegarver and C. T. Chen. 1985. NOAA Technical Memorandum. ERLPMEL-60, 46 pp.
(16) Poisson, A. and C. T. Chen. 1987. *Deep-Sea Res.*, **34**, 7, 1255–1275.
(17) Shiller, A. M. 1981. *J. Geophys. Res.*, **86**, 11,083–11,088.
(18) Broecker, W. S., T. Takahashi and T.-H. Peng. 1985. DOE Tech. Rep., DOE/OR-857, 79 pp.
(19) Fine, R. A., J. L. Reid and H. G. Ostlund. 1981. *J. Phys. Oceanogr.*, **11**, 3–14.
(20) Reid, J. L. 1965. Johns Hopkins Oceano. Studies No. 2, 85 pp.
(21) McCartney, M. S. 1982. *J. Mar. Res.*, **40**, supplement, 427–464.
(22) Sarmiento, J. L., J. C. Orr and U. Siegenthaler. 1991. *J. Geophys. Res.*, in press.
(23) Wang, S. L. 1988. MS Thesis, Inst. Mar. Geol. Sun Yat-Sen Univ. Kaohsiung, Taiwan, ROC, 122 pp. (in Chinese).
(24) Wyrtki, K. 1981. *J. Phys. Oceanogr.*, **11**, 1205–1214
(25) Ostlund, H. G., R. Brescher, R. Oleson and M. J. Ferguson. 1979. Tritium Lab. Data Rep. 8, Univ. of Miami, 384 pp.
(26) Van Scoy, K. A., R. A. Fine and H. G. Ostlund. 1991. *Deep-Sea Res.*, **38**, Suppl. 1, S191–S219.
(27) Broecker, W. S., R. Gerard, M. Ewing and B. H. Heezen. 1960. *J. Geophys. Res.*, **65**, 2903–2931.
(28) Broecker, W. S. 1963. *The Sea*, Vol. 2, M. N. Hill (ed.), Interscience, pp. 88–108.
(29) Druffel, E. M. 1980. Ph.D. Thesis. University of California at San Diego, La Jolla, 213 pp.
(30) Toggweiler, J. R. 1983. Ph.D. Thesis. Columbia University, 403 pp.
(31) Ostlund, H. G. and M. Stuiver. 1980. *Radiocarbon*, **22**, 25–53.
(32) Gamo, T., Y. Horibe and H. Kobayashi. 1987. *Radiocarbon*, **29**, 1, 53–56.
(33) Chen, C. T. 1991. *Cont. Shelf Res.*, in press.